Design of a low-temperature solar heating system based on a slurry Phase Change Material (PCS)

Post-print of the article:
Design of a low-temperature solar heating system based on a slurry phase change material (PCS)
by Gianluca Serale, Enrico Fabrizio, Marco Perino
Doi: 10.1016/j.enbuild.2015.06.063 published in *Energy & Buildings*, vol 106 (2015), pp- 44-58

Design of a low-temperature solar heating system based on a slurry phase change material (PCS)

Gianluca Serale[a], Enrico Fabrizio[b*], Marco Perino[a]

[a] *Dipartimento Energia (DENERG), Politecnico di Torino, Corso Duca degli Abruzzi 24, 10129 Torino, Italy*

[b] *DISAFA, Università degli Studi di Torino, L.go Paolo Braccini 2, 10095 Grugliasco (TO), Italy*

*Corresponding author: Tel: +39-011-670-5525, fax: +39-011-670-5516, e-mail: enrico.fabrizio@unito.it

Abstract

Flat-plate solar thermal collectors are the most common devices used for the conversion of solar energy into heat. Water-based fluids are frequently adopted as heat carriers for this technology, although their efficiency is limited by certain thermodynamic and heat storage constraints. Latent heat, which can be obtained from microencapsulated Phase Change Slurry (mPCS) - that is a mixtures of microencapsulated Phase Change Materials (mPCM), water and surfactants - is an innovative approach that can be used to overcome some of the aforementioned limitations. The viscosity of these fluids is similar to that of water, and, as a result, they can be pumped easily. Some of the thermo-physical and rheological properties and the material behaviour of flat-plate solar thermal collectors with an mPCS as the heat carrier fluid are analysed in the present work. Solar thermal systems filled with an mPCS are proposed and a prototypal system is presented. The possible advantages and drawbacks of this technology are also discussed.

Keywords: renewable energy sources, solar collector design, phase change slurry (PCS), thermal storage, solar thermal system, latent heat storage.

Nomenclature

Symbols

a	mass percentage	[-]
c_p	specific heat at constant pressure	[kJ kg^{-1} K^{-1}]
h	specific enthalpy	[kJ kg^{-1}]
$\dot{m}$	mass flow rate	[kg m^{-1}]
r	latent heat	[kJ kg^{-1}]
t	time	[s]
A	area	[m^2]
D	diameter	[m]

G_T	global irradiance	[W m^{-2}]
$\dot{Q}_u$	useful thermal power	[W]
T	temperature	[°C]
η	efficiency	[-]
ρ	density	[kg m^{-3}]

Subscripts

avg	average temperature in the storage tank
collector	solar thermal collector
core	core of the micro-encapsulated Phase Change Material
in	solar thermal collector inlet
inf	inferior limit of the phase change
H_2O	water as heat transfer fluid
m	mean
n	nominal
out	solar thermal collector outlet
outdoor	outdoor environment
shell	shell of the micro-encapsulated Phase Change Material
sup	superior limit of the phase change
TC16	heating system supply temperature
TC18	heating system return temperature

Abbreviations

DHW	Domestic Hot Water
DSS	Demand Side Simulator
HTF	Heat Transfer Fluid
mPCM	micro-encapsulated Phase Change Material
mPCS	micro-encapsulated Phase Change Slurry
PCM	Phase Change Material
PCS	Phase Change Slurry

1. Introduction

Energy consumption in the building sector has become one of the most important entries of total energy consumption and CO_2 emissions in developed countries (e.g. in the EU about 40% of the consumed energy and the produced CO_2 is related to buildings) [1]. Much of this increased energy use is due to increases in the standard of living and in thermal comfort. In order to satisfy these requirements, the consumption of active systems has been increasing in parallel [2]. In a sustainable approach, the energy demand needs to be reduced and an improved exploitation of renewable energy sources has to be introduced.

A recent study, carried out at the end of 2011 [3], has reported that the worldwide installed heating capacity produced using solar thermal collectors is about 234.6 GWth, which

corresponds to a total of 335.1 million square meters of collector area in operation. Solar thermal collectors are the most common devices used to convert solar energy into heat. Conventional collectors generally use water and an additive (usually glycol, which acts as an antifreeze) as a Heat Transfer Fluid (HTF). This technology has been investigated extensively since the '40s [4].

The solar thermal market in Italy is constituted by around 400,000 m^2 of panels installed each year, and the total installed capacity of thermal solar exceeds 1 GWt. (Assolterm - Italian Association of Solar Thermal). However, compared to other European countries, Italy is behind with respect to both the total installed capacity per capita (18 kWt per 1,000 inhabitants, compared to the 270 kWt per 1000 inhabitants of Austria), and the annual market (with an installed capacity of 5 kWt per 1,000 inhabitants, compared to the 29 kWt per 1000 inhabitants of Austria). Of all the solar thermal systems installed in Italy, 90% serves for the production of domestic hot water (DHW), while space heating and DHW combisystems are not very common; 85% of the installed solar collectors is of the flat glazed type, and vacuum tube collectors represent only 15% [5].

Water solar collectors, despite having been the subject of extensive studies and having undergone a technological evolution over the last few years that has improved energy efficiency (in particular by improving the solar collector evacuated tube technology and employing heat pipe technology), still suffer from some limitations [6].

First, since a heating demand occurs when no or low solar energy is available, the exploitation of solar energy for space heating purposes through traditional collectors is not often profitable, or it at least requires large storage systems. In fact, there is a time mismatch between solar energy availability and energy demand [7]. The time delay between the availability of energy and its consumption is one of the most important problems in renewable energy applications [8]. In winter time, the limited solar irradiation can barely cover the total energy demand for heating. On the other hand, no direct profitable use has been found for the high solar energy that is available in summertime, which can be converted by solar collectors, unless huge and expensive seasonal storage strategies are adopted [9].

Secondly, there are some energy losses and drawbacks due to the relatively high working temperatures of the HTF. The HTF plays a very significant role in a solar thermal system, because it is used to transfer the energy absorbed in the collector to the heat exchanger placed inside the storage tank. The working temperatures of the HTF are reached through the adoption of traditional solar thermal systems based on water solutions. A typical range required to

provide heat terminal units with a sufficiently large enthalpy flux and reasonable flow rates so that sufficiently small energy storage systems can be used is 50-60°C. This relatively high HTF temperature range causes two different sets of problems:

- The first set of problems is related to the considerable thermal energy losses that occur in all of the system components. These are due to the high temperature difference between the HTF and the environment. For this reason, an increase in this temperature difference corresponds to a decrease in the instantaneous system efficiency as well as in the seasonal system efficiency. Higher efficiencies are only reached for a fixed HTF temperature when the environment temperature rises. Once again, in winter time, when the temperature and irradiance are lower, the capability of the solar thermal system to exploit solar energy is reduced. Even in those winter days when there is high irradiation, the water-based HTF undergoes a relevant increase in temperature to exploit the solar energy, and the inefficiency of the process also increases due to the enhanced heat dissipation towards the outside.
- The second set of problems is related to the time variation of the short periods of time during which the solar thermal system can be exploited to produce heat. Generally, the higher the HTF temperature, the higher the minimum irradiation required to produce a useful heat gain [10].

An interesting concept to overcome the limitations of the present-day flat plate technology involves the exploitation an HTF that uses the latent heat instead of (or in combination with) the sensible heat. In recent years, several research projects, involving a two-phase heat transfer process [6], have been conducted to study the effectiveness of solar thermal systems. In this way, the isobaric phase change process within the HTF occurs at an almost constant temperature, without compromising the ability of the system to store thermal energy. Therefore, solar energy is exploited at lower thermal levels, and the previously described problems, due to a relatively high temperature range, are also reduced. The use of refrigerant-filled solar collectors, whose application dates back to the ‘70s, has been investigated by many researchers. In these studies, heat pumps, integrated with solar collectors, were used to exploit the phase change of the refrigerants that were used as the HTFs. Many kind of refrigerants - such as CFC, HCFC and HFC [11, 12] - or other natural fluids – such as propane or CO2 – have been used successfully [13, 14]. Generally, when operating in a transcritical condition, the efficiency of these solar thermal systems is much higher than that of traditional water-based collectors. Nevertheless, these technologies are not so widely diffused due to the presence of substances

that are harmful to the environment and to the complexity of the system.

1.1 Literature review on the adoption of Phase Change Materials (PCMs) in solar thermal applications

All the previous attempts mentioned exploited the liquid-to-gas transition latent heat of an HTF. However, it is also possible to exploit the solid-to-liquid transition latent heat. This can be obtained through the introduction of PCMs into the solar system. These materials have a high latent fusion heat and an appropriate melting point for the application. PCMs are able to store excess energy, that/which would be otherwise wasted, and to match the demand and supply when they do not coincide in time [15, 16]. They have recently become a widespread adopted solution in various building applications [17 – 21], including solar thermal system components. The substances used as PCMs can be organic (such as paraffin and fatty acids), or inorganic (such as hydrate salt solutions); both show a single melting temperature when they are pure, and a melting range when they are mixtures [22]. They act like an almost isothermal heat reservoir, due to the large amount of heat they absorb or release during their phase transition.

In the past few years, the use of PCMs has been tested in several different types of solar thermal systems. The presence of a PCM leads to an overall annual increase in the solar fraction, a higher efficiency of the system and major storage heat capacity. Three different methods in particular have been proposed to incorporate PCMs into systems: the integration of a PCM directly in a layer of the solar collector, the addition of PCM nodes to the primary HTF solar loop pipes and the addition of PCM elements to the inside of a storage tank [2].

In the first kind of proposed collectors (Figure 1(a)), the PCM is integrated directly as the storage function. In the most common configuration, the PCM-integrated solar collector eliminates the need of conventional storage tanks, thus reducing costs and space. For example, in [23], the solar energy is stored in a salt-hydrate PCM layer held in the collector, and is discharged to cold water flowing through a surface heat exchanger located in an upper layer. A similar concept, which proposes a different kind of PCM and layer organization to obtain better energy storage in the collector, has recently been introduced in [24 – 26]. A thermal solar system with PCS storage integrated in the collector has been studied in [27]. The storage-collector was filled with different concentrations of PCS with a 60°C phase transition temperature. On the other hand, in [28], a PCM layer has been incorporated in a collector which combines PV and solar thermal functions. This is principally to improve the inertia of the system in order to limit the temperature peaks and increase the PV efficiency without wasting

energy [29].

A new system configuration (Figure 1(b)) has been proposed in [30] and [31]. It has been called SDHW–PCM, and it includes a PCM node in the HTF primary solar loop of the system. The node is combined with a traditional water storage tank, and it represents an additional storage unit. It is a compact heat exchanger made of four plates surrounded by storage composite material composed of compressed expanded graphite (CENG) and paraffin. The authors showed that, compared to a traditional water based solar thermal system, this configuration leads to increases in the solar fraction (i.e. the time during which the solar thermal system can be exploited to produce heat) in summer and in winter of 8% and 4%, respectively.

The third kind of proposed solar thermal systems (Figure 1(c)) are those that use PCMs in the storage tank. A study on the enhancement of solar system performance using sodium thiosulfate pentahydrate as the PCM in the storage tank has been made by [32]. They found that the storage time was approximately 2.59–3.45 times greater than that of conventional water-heating systems. Experiments that involved the inclusion of a water tank and a PCM module in a complete solar water heating system have been conducted in [33] and in [2]. In this case, the PCM was placed in several cylinders at the top of the water tank. However, to date, the direct use of PCMs for energy storage and/or heat transfer applications has been limited, due to the low thermal conductivity of most PCMs, particularly when they solidify on the heat transfer surface.

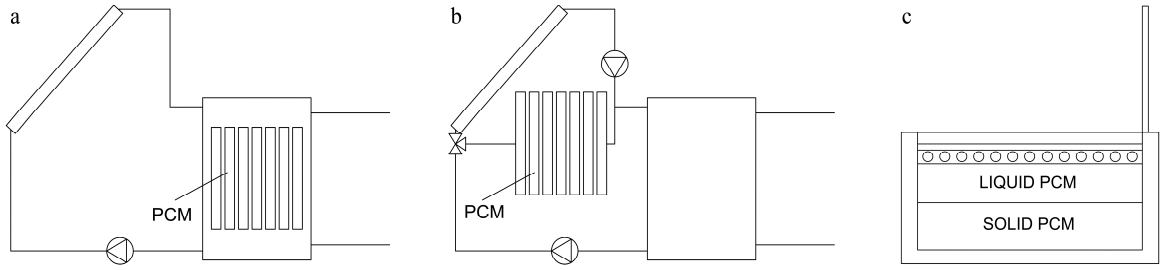

Figure 1 Examples of PCM integration into solar thermal systems: PCM integrated into the storage tank (a); PCM node between the collector and the storage tank (b); PCM integrated into the solar collector (c).

Most of these solutions have only considered the improvement of a single static component of the solar thermal system. However, the HTF plays a very significant role in a solar thermal system. It absorbs energy in the collector and transfers it through the heat exchanger to the storage tank. All of the so far proposed solar thermal systems have used water or water-glycol as the HTF in the primary loop of the solar collector. Nevertheless/However, this strategy

implies exchanges with fixed temperature differences between the HTF flowing inside the solar collector loop and the PCM storage, as well as between the storage and the HTF flowing to the terminal units. These heat exchanges introduce irreversibility and energy-exergy losses. Moreover, in recent years, the thermal capacity of HTF – that is the amount of heat transported by a unit of flow rate of HTF – has also been considered an important problem. Many thermal-energy systems have long piping sections to convey the HTFs from the source to the sink heat exchangers. In such conventional systems, thermal energy is transferred as the sensible heat of the HTF, and it is proportional to the difference between the source and the sink temperatures. If the temperature difference is small (as in the case of many renewable energy sources), the single-phase fluid must be pumped at high-volume flow rates. As a result, the system consumes a large amount of pumping power.

1.2 Literature review of Phase Change Slurries (PCSs) in solar thermal applications

All the previous problems led Kasza at al. [35] to propose a system that directly uses PCMs inside water based suspensions, called PCS [22, 36], as an enhanced HTF in the primary loop of solar collector systems. Nevertheless, during the 80's, some technological limitations arose, due to the possible solidification of the slurry in the pipes during its phase transition. Currently, due to the advancements in PCM technologies, an alternative solution could be conceived. In fact, 5 different types of PCS can nowadays be identified, that is: ice slurries, PCM microemulsions, microencapsulated PCM slurries (mPCS), clathrate hydrate PCM slurries and shape-stabilized PCM slurries [22].

In order to meet Kasza's demand for an HTF, that always remains in liquid form to ensure the circulation of the slurry in the pipes, an mPCS could be used. This mPCS is a mixture of a micro-encapsulated PCM suspended in water and glycol or other HTFs. In this way, the two-phase fluid has almost constant rheological properties, and the phase change only concerns the core of the microcapsules. The mPCS always remains liquid, although it has a high viscosity, and it can be pumped regardless of its state of aggregation.

Recently, mPCSs have been studied extensively in literature and in laboratory experiments, due to the reduced problems of clogging in the pipes and the reduced production costs of the material [2, 22]. In these slurries, the mPCM (generally paraffin) is encapsulated in a core within a thin film to form microcapsules, and is then suspended in a carrier fluid (generally water or water and glycol). Microencapsulation is a process by which tiny particles or droplets are surrounded by or coated with a polymer film. Microencapsulation processes were developed

above all by pharmaceutical industries, and different microencapsulation methods are available, such as in-situ polymerisation and interfacial polycondensation [38]. The advantages of using mPCSs in different thermal applications have been clear since the late '90s [22, 39]. First, the main benefit is that they always remain in liquid form and can be pumped as an HTF with high thermal capacity. Moreover, an mPCS can serve as the thermal storage media and as the HTF, and hence many potentially important applications are possible. For instance, in [34], an mPCS thermal energy storage was proposed in a residential solar energy system. The mPCS enhances the heat transfer capacity of the PCMs and still retains the characteristic of high-energy storage density over a small temperature range.

Furthermore, in this form, the same medium can be used to both transport and store energy, hence reducing the heat transfer losses due to energy exchanges. On the other hand, an mPCS allows the heat transfer rate of the material to be increased by raising the surface to volume ratio. Furthermore, they have a high storage capacity during the phase change, and heat transfer occurs at an approximately constant temperature [36]. Eventually, the isothermal storage energy process with a phase change allows the thermal energy losses from the HTF to the environment to be reduced. To actually take advantage of the mPCS properties, the following requirements are necessary: the phase change temperature range has to match the application, low pressure drops have to occur in the pumping system, the mPCS has to be stable under both thermal and mechanical loads, the capsules must not leak and the pipes must not clog [37].

However, the use of mPCSs also involves some drawbacks. For example, it is impossible to exploit the latent heat if the phase change temperature of the material is not chosen correctly to match the temperature range of the application. Moreover, the viscosity of the mPCS is generally higher than that of water [36]. Viscosity could become much higher than water for high concentration suspensions and an increase in the pressure drops could occur [38]. Furthermore, the mPCS might not remain physically stable in certain conditions. For example, some creaming phenomena could occur under certain conditions, and the pipes could clog [37, 40]. The thermal and mechanical loads, such as the mechanical stress generated by the circulating pump, could eventually damage the microcapsule and the material could leak outside the capsule shell. During the last few years, most of these problems have been studied extensively, and different solutions have been proposed to solve these drawbacks [41].

In spite of these studies, the literature analysis has revealed a lack of evidence concerning the advantages and disadvantages of the exploitation of the transition of solid-to-liquid latent heat in combination with solar collectors. Therefore, a dedicated experimental study was set up, and

it is currently ongoing, with the aim of obtaining more detailed knowledge and understanding of such a technology.

1.3 Scope of the work

In order to try to overcome the drawbacks of traditional solar thermal systems, a new solution, based on mPCS, has been conceived, designed and prototyped. The basic idea was to create a system that would be able to directly use an mPCS as a heat carrier fluid and as an energy storage medium.

The use of PCS as the HTF, instead of traditional aqueous solutions, makes it possible to exploit the effect of latent heat, to improve the flexibility of the solar thermal system, and to thus increase the efficiency of solar collectors and energy storage systems. Compared to other solutions (with reference to PCM) that are already available on the market, such as heat pipes, the proposed configuration would in principle allow greater flexibility, in relation to variations in the boundary conditions or energy demand profiles, and would allow the heat transfer between different components to be limited (thus improving the overall energy efficiency of the system). Systems based on heat pipes and heat pipe collectors exploit the liquid - vapor phase change and allow the heat transfer to be optimized, while they do not allow energy to be stored (at least not exploiting a given and fixed temperature difference).

In the proposed solution, the mPCS based fluid has the characteristic of being able to remain in motion, regardless of the state of the PCM (solid/liquid), thus making it possible to store thermal energy directly in the fluid and, therefore, to utilize the entire mass of the fluid in the pipes and not only in the "storage tank".

The proposed technology, compared to the existing solutions on the market, differs as far as the following aspects are concerned:

- it offers the ability to operate at low thermal levels with satisfactory efficiencies (thus improving the manufacturability of the panels);
- it results in a reduction in heat losses due to transmission, thanks to the lower temperature differences;
- it offers the possibility of using analogous, or very similar components to those of traditional water systems;
- it offers the possibility of relatively low costs of the fluids (in comparison to other methods) and easy maintainability;
- it offers the possibility of adapting the system for summer cooling.

The characterization and the performance of the system are presented and evaluated hereafter through a comparison with those of a reference (conventional) collector. It is worth mentioning that the conceived mPCS based system includes a PCM-based heat storage unit coupled with a solar collector and a secondary, water-based circuit, in order to supply heating to the indoor environment.

2. Design of the prototype

A solar thermal system designed for space heating is here proposed. In general, two possible system configurations can be adopted. The first one, which is represented in Figure 2(a), consists of a two open-loop circuit filled with mPCS. In this case, both the solar primary loop and the space heating secondary loop use mPCS as the HTF. The complete absence of fixed temperature differences between the two loops guarantees the maximum theoretical thermal efficiency from an exergetic point of view. The main drawback of this configuration concerns the difficulties that arise, from a technological point of view. The mPCS is an HTF which has different rheological properties from water, and it requires special attention during pumping, especially at the users' side.

The system described in Figure 2(b) solves some of these problems by reducing the length of the pipes in which the mPCS flows. It consists of a solar primary loop filled with an mPCS, coupled with a closed heating system secondary loop filled with water. As in the previous solution, the storage tank contains an mPCS, and it allows large amounts of energy to be stored. However, the temperature difference between the storage tank and secondary water loop leads to a slight reduction in efficiency. On the other hand, this system guarantees easier technological implementation and it allows a better evaluation of the behaviour of the solar system filled by mPCS. For these reasons, the solution shown in figure 2(b) was adopted by the authors as the most suitable to set up the prototype.

Various steps were necessary to properly design and build the system. Firstly, a specific research was conducted to identify the most suitable mPCS to be used as the HTF. Secondly, the components of the system (solar collector, primary loop pipes, pumps, storage tank) were designed. Finally, in order to be able to experimentally test the system under realistic operative conditions, a heating demand side simulator (DSS) was conceived and built.

Post-print of the article:
Design of a low-temperature solar heating system based on a slurry phase change material (PCS)
by Gianluca Serale, Enrico Fabrizio, Marco Perino
Doi: 10.1016/j.enbuild.2015.06.063 published in *Energy & Buildings*, vol 106 (2015), pp- 44-58

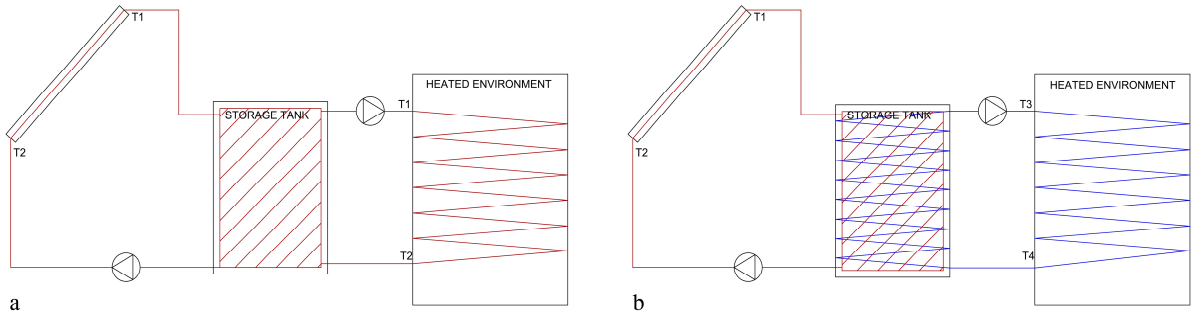

Figure 2 Schematics of the prototype: a two open-loop circuit (a); an open-loop circuit with mPCS and a closed-loop circuit with water (b). mPCS highlighted in red, while water highlighted in blue.

4.1 Selection and characterisation of the primary HTF

The mPCS is a suspension of two components: a carrier fluid and a suspended material. The carrier fluid is a mixture of water and glycol. The mass percentage of the glycol was determined on the basis of the average local climate conditions in Torino (where the prototype was installed and tested) . A 40% weight concentration of glycol was used for this mock-up. Table 1 describes the main thermo-physical properties of the carrier fluid:

Table 1. Heat transfer carrier (water + glycol) properties.

Specification	Symbol	Value	M.u.
Mass percentage of glycol	a_{gl}	40.0	%
Mixture (water+glycol) density	ρ_{w+gl}	1044	kg m^{-3}
Mixture (water+glycol) specific heat	cp_{w+gl}	3600	J kg^{-1} K^{-1}
Mixture (water+glycol) conductivity	λ_{w+gl}	0.369	W m^{-1} K^{-1}

The suspended material is an mPCM. Many types of mPCM are available on the market [37]. The one with the most suitable phase change temperature range was chosen. In order to minimise the heat losses and to increase the instantaneous efficiency of the system, the most suitable range was chosen as the lowest possible for the application. This is the range that allows heat exchange with the various components of the system. For example, in low temperature radiant panels, the minimum thermal storage temperature that allows heat exchange with the secondary heating loop is between 35 °C and 40 °C. An mPCS based on n-eicosane mPCM was chosen to match this temperature range [44]. The n-eicosane phase change range is 36 ° - 38 °C. Many of the data on properties of the mPCM contained in the bulk of the microcapsules can be found in literature [46, 47] while others have been provided by Microtek Laboratories [45], the manufacturer of the material. Table 2 summaries the main thermo-

physical properties of the mPCM n-eicosanes available in literature.

Table 2. Thermo-physical properties of the n-eicosane.

Specification	Symbol	Value	M.u.	Reference
Mass percentage of the core	a_{core}	87.5	%	[45]
Core density (solid/liquid)	ρ_{core}	815/780	kg m^{-3}	[46]
Shell density	ρ_{shell}	1190	kg m^{-3}	[46]
Average particle diameter	D_{mPCM}	$17\text{-}20\cdot10^{-6}$	m	[45]
Conductivity (solid/liquid)	λ_{mPCM}	0.23/0.15	W m^{-1} K^{-1}	[46]
Specific heat (solid/liquid)	c_{p_mPCM}	$1.92/2.46\cdot10^{3}$	kJ kg^{-1} K^{-1}	[46]
Latent heat	r_{mPCM}	$1.95\cdot10^{5}$	kJ kg^{-1}	[45]
Nominal phase change temperature	T_{n_mPCM}	37	°C	[45]
Phase change range	T_{inf_mPCM}-T_{sup_mPCM}	36-38	°C	[47]

Although the mPCM bulk material characteristics only depends on the chosen material, as shown in Table 2, the overall properties of the mPCS are functions of the concentration of its components. The mPCM-to- water glycol concentration ratio influences both the thermo-physical and rheological properties of the mPCS; the latter show highly non-linear behaviour. The choice of the concentration ratio affects the relation between the pumping work and the heat transfer, which is very important to obtain energy savings [48]. A compromise between these two characteristics should be reached. This compromise is a trade-off, since improving one characteristic may deteriorate the other one. On one hand, a high concentration of mPCM improves the heat transfer characteristics of the material, while on the other hand it increases the viscosity of the fluid and the pumping energy demand. However, a higher thermal storage capacity also implies a lower flow rate and hence a reduction in the electric energy demand from the pump [49]. Once the optimised concentration has been chosen, the properties of the whole suspension can be calculated using formulations available in literature [50 - 52].
After microencapsulation, the enthalpy of the melting will decrease and the pure n-eicosane values will no longer be valid. However, a particular feature of mPCSs is that their thermo-physical properties are not only functions of the mPCM but also of its concentration. For this reason, a characterisation of the mPCS is necessary, and the definition of the specific enthalpy-temperature curve, for various concentrations, is an important step in this procedure [53]. A T-History method [54] was used to determine these thermo-physical properties. The specific enthalpy-temperature curve that resulted from the elaboration of the measured data for mPCM concentrations of 30 wt. % and 40 wt. % is reported in Figure 3. The specific enthalpy of pure distilled water was taken as a reference for comparison purposes, and it is reported in the chart

with a dashed line. The specific enthalpy was set equal to 0 J/kg at 20 °C for each sample in order to have a reference value. Tests were performed by cooling the samples and the resulting melting range (36.5 – 34.5 °C) was a little lower than the one reported in the literature and technical sheets. From this experiment, it results that the specific enthalpy of solidification for a 30 wt. % concentration of n-eicosane mPCM is almost 48 kJ/kg, while for a 40 wt. % concentration of n-eicosane mPCM it is almost 62 kJ/kg. The chart reported in Figure 3 highlights the temperature range close to the phase change (30 °C – 40 °C). However, a small amount of phase change enthalpy, which is due to rotator-crystal transition [47], appears in the temperature interval below 30 °C (not shown in the figure).

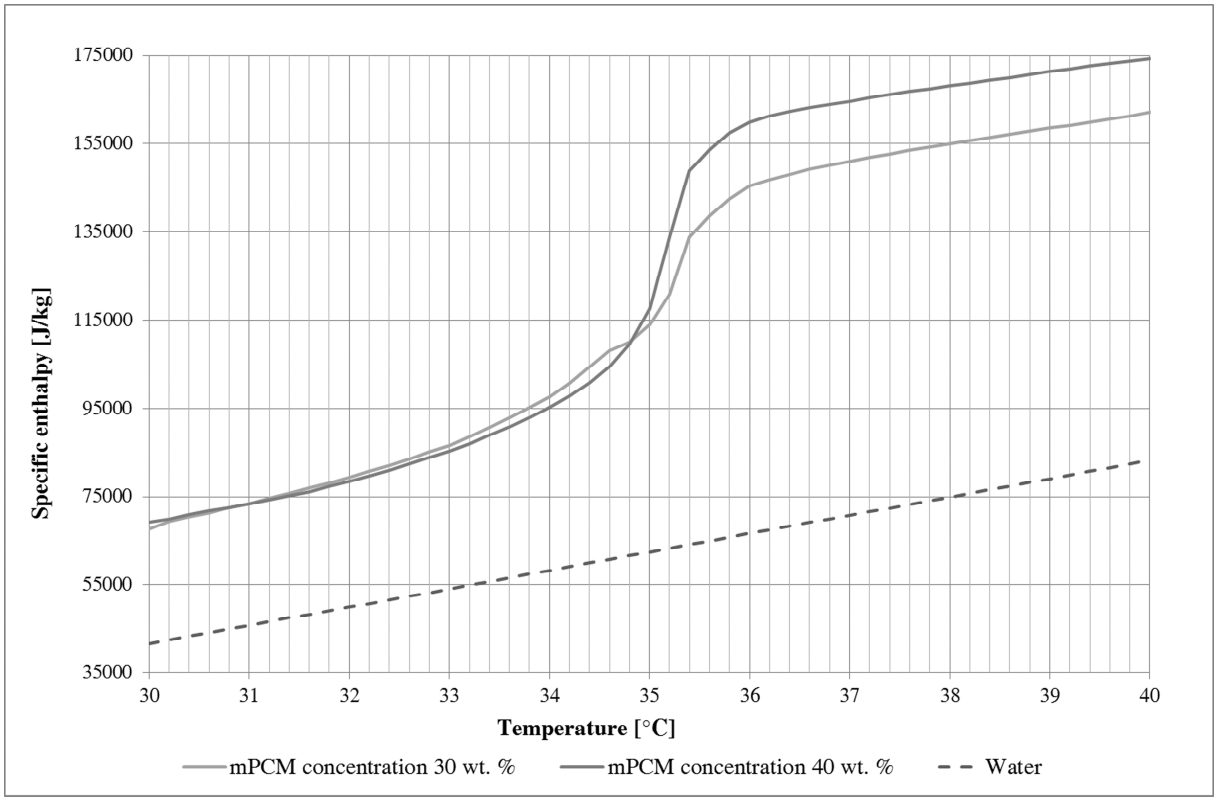

Figure 3 Results of T-history method experiments to determine the specific enthalpy versus temperature for 30 wt. % and 40 wt. % mPCM concentration.

Several pressure drop tests have been carried out using different concentrations of mPCM before the real scale prototype system was set up. The pipe circuit shown in Figure 4 was used to perform the tests. This real-scale circuit is made up of similar copper pipes to those used in flat-plate solar collectors. The inner diameter of the pipes is 8 mm and the external diameter is 10 mm. Four inspection piezometer pipes were placed in the circuit to monitor the distributed pressure drops. Different kinds of tests were carried out. First, the circuit was tested using water

with glycol to simulate the typical HTF used in solar thermal systems. In this case, the results obtained for the distributed pressure drop were similar to typical literature values.

Figure 5a shows the outcomes of a pressure drop test for different volume flow rates at a 40 wt. % concentration of mPCM. Previous/Other enthalpy-temperature tests had individuated this concentration as the most promising for the heat storage capacity of the material. Furthermore, the test reported in Figure 5b shows the variation in the pressure drop as the mPCM concentration in the mPCS solution is increased. The volume flow rate was set to a typical constant value of solar applications, that is, equal to 30 l h^{-1} ($8.33 \cdot 10^{-6}$ m^3 s^{-1}). The circuit was tested using mPCSs with different mPCM concentration values: 25 wt. %, 30 wt. %, 35 wt. %, 40 wt. % and 45 wt. %.

An interesting outcome from these tests is that the monitored pressure drop varies in time. In fact, after 12 hours of monitoring, the material shows completely different behaviour with a less pronounced pressure drop. The higher the mPCM concentration, the higher this phenomenon appears. This is principally due to the appearance a division in layers in the mPCS with different micro-capsules concentrations, which is known as the creaming phenomenon and treated in section 4.3 of this paper.

The mPCS viscosity and pressure drop in these tests resulted to be similar to those of water for lower mPCM concentrations than 30 wt. %. A non-linear increase in the viscosity occurred for concentrations of up to 35 wt. % - 50 wt. %. The mPCS could not be pumped for higher concentrations than 50 wt. %. The results were compared with literature values and rheometer tests.

Post-print of the article:
Design of a low-temperature solar heating system based on a slurry phase change material (PCS)
by Gianluca Serale, Enrico Fabrizio, Marco Perino
Doi: 10.1016/j.enbuild.2015.06.063 published in *Energy & Buildings*, vol 106 (2015), pp- 44-58

Figure 4 Experimental setup for pressure drops determination.

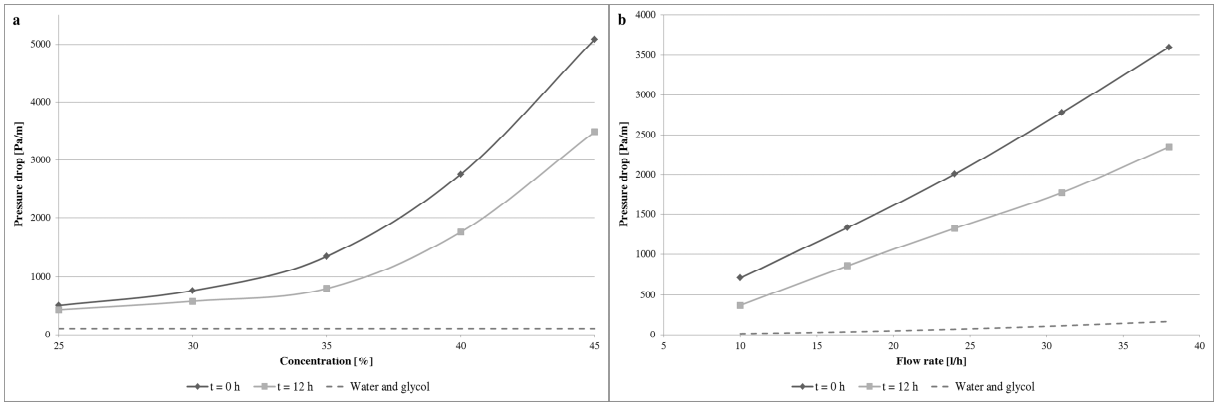

Figure 5 Results of pressure drop tests for different concentrations of mPCM at the constant flow rate of 30 l h^{-1} (a). Results of pressure drop tests for different flow rates at 40 wt. % concentration of mPCM (b).

4.2 *Solar collector*

Once the rheology tests had demonstrated that, up to a certain viscosity, the mPCS could flow in the pipes of flat-plate solar collectors, the specifications of the panel were chosen. In a future development of the system, the optimization of the hydraulic circuits could be considered, but, at present, thanks to the fact that the rheological properties of the fluid used for the prototype are not so different from those of a typical glycol-water solution, a commercial solar thermal collector has been adopted for the measurement campaign. The main features of the chosen collector are summarised in Table 3:

Table 3. Specification of the solar thermal collector.

Specification	Symbol	Value	M.u.
Panel length	L	2.1	m
Panel width	l	1.1	m
Panel thickness	s	0.20	m
Number of heat exchanger pipes	N_{pipes}	8	-
Distance between heat exchanger pipes	W_{pipes}	0.13	m
External diameter of pipes	D_{pipes}	0.008	m
Inner diameter of pipes	d_{pipes}	0.0076	m
Plate thickness	s_{plate}	0.0002	m
Plate absorbing coefficient	α_{plate}	0.95	-
Plate emissivity	ε_{plate}	0.05	-
Plate conductivity	λ_{plate}	385	$W\ m^{-1}\ K^{-1}$
Bond width	l_{bond}	0.0002	m
Cavity thickness	s_{cavity}	0.025	m
Cover thickness	s_{caover}	0.004	m
Cover extinction coefficient	K_{caover}	16.10	m^{-1}
Air refraction index	n_1	1	-
Cover refraction index	n_2	1.526	-
Cover emissivity	ε_{cover}	0.8	-
Thickness of the bottom insulation	s_{ins_bot}	0.05	m
Thickness of the edge insulation	s_{ins_edg}	0.02	m
Insulation conductivity	λ_{ins}	0.04	$W\ m^{-1}\ K^{-1}$

4.3 Primary loop and storage

Many examples of PCSs based storage tanks for solar systems can be found in the literature [34, 55]. One of the main disadvantages of latent heat storage systems is the low thermal conductivity of many PCMs, which causes poor melting and solidification rates. Many solutions have been proposed to solve this problem [56- 59]. Since the first set of tests was planned to focus on the behavior of the flat plate panel and the whole circuit, a traditional inertial storage tank with a spiral heat exchanger was chosen. The volume of the storage tank is 200 l and the

operating pressure 3 bar. The spiral heat exchanger has many by-pass possibilities in order to choose the heat exchange surface (whole storage tank, upper part, lower part). Specific measures concerning the geometric optimization of the tank may be adopted in the future. However, during the preliminary tests on the material, another problem arose: when the fluid was not in motion, – for example, in the storage tank during the off periods - a creaming phenomenon occurred. Creaming is the movement of mPCM particles towards the upper part of the suspension as a result of gravity [37, 62]. In the case of the n-eicosane mPCS, the creaming is due to the density difference between the suspended material and the carrier fluid. As a result of creaming, a layer with a higher concentration of mPCM occurs in the upper part of the suspension. This kind of process is quite common in mPCSs, and it usually takes hours or even days to overcome. However, very few studies on this phenomenon are available in literature, although a detailed investigation on the physical stability of PCSs was carried out by Delgado et al. [40]. In general, creaming can be solved by reducing the mPCM capsule size or by adding surfactants [37]. Al-Shannaq et al. [60] increased the stability of a PCS with a poly methyl methacrylate shell using mixed surfactants, such as SDS and PVA. Zhang & Zhao [59] dealt with the problem of mPCS creaming by adding multi-walled carbon nanotubes. The mPCS showed good stability and no visible creaming or sedimentation were observed two months after the addition of the nanotubes. A study on an mPCS conducted at the Fraunhofer Institute for Solar Energy Systems has been reported in [60]. In this case, a thickener was added to the mixture and this slowed down the separation speed.

In order to have visual control of the creaming, 12 inspection openings were made in the prototype storage tank. Moreover, the mPCS was continuously kept in motion in the storage tank, even during the off periods. This was made possible through the use of partitions in the storage tank (which can be seen in Figure 6 and of a bypass circuit, with a second peristaltic pump, which is switched on when the main pump of the primary loop is stopped. This process causes additional energy consumption and makes the pumping system more complex. Furthermore, if the mPCS is mixed continuously, the HTF in the storage tank cannot stratify and the heat transfer to the secondary loop becomes worse. However, at this stage, the adoption of a bypass circuit was chosen because it was the easiest and cheapest way to overcome the creaming phenomenon. It would in fact have been possible to find a chemical-physical solution for the creaming problem, but such a study was beyond the scope of this work, although it may be dealt with in the future, before the system is put on the market.

Furthermore, it should be noted that, on the one hand, the electric energy consumption of the

auxiliary recirculation pumps is expected to be very low (as the speed of the fluid is kept quite low in order to avoid the creaming process) while, on the other, the control strategies of the system will be aimed at optimizing the exploitation of the latent heat of the system; therefore, for most of the time the fluid will be roughly isothermal and stratification in the storage tank will not take place.

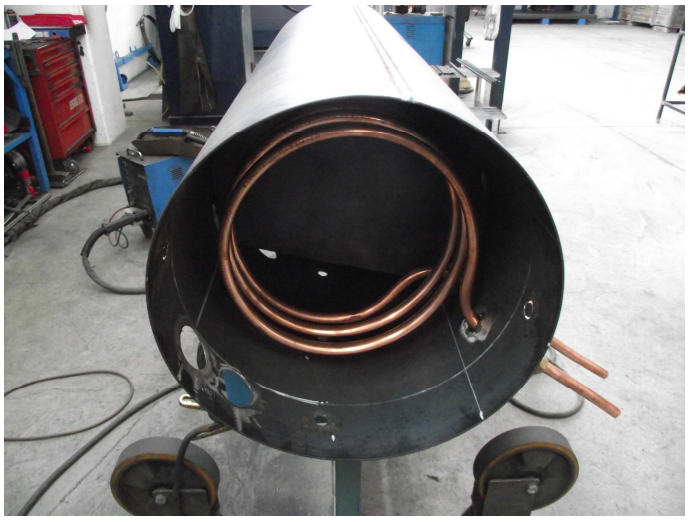

Figure 6 View of the interior of the storage tank and the heat exchanger.

4.4 Primary loop pump selection

Rupture of the mPCM microcapsules can cause several problems to the system. In particular, leakage of the PCM from the capsule could induce clogging of the pipes and a change in the thermal properties of the HTF. Damage and cracking of the capsules are usually due to mechanical stress induced by the pump [63]. Centrifugal pumps do not generally induce capsule rupture, and only a small number of microcapsule shells has been damaged or destroyed during long-term operations [64, 65]. However, peristaltic pumps were adopted to avoid such problems. These pumps offer the advantage of not having any moveable parts in direct contact with the fluid that flows inside the pipe. Therefore, there are fewer mechanical actions than in any other kind of pump. The main pump of the primary loop, which is a programmable Verderflex Scientific AU UV 3000 HD, whose main features are summarized in Table 4, is shown in Figure 7.

Table 4. Specifications of the Verderflex Scientific AU UV 3000 HD pump.

Specification	Value	M.u.
Power consumption	100	VA

Protection rating	IP66	-
Speed control	4-20	mA
	0-10	V
Speed range	10-250	RPM
Standard tube material	verderprene	-
Standard tube inner diameter size	0.0080	m
Standard tube inner diameter thickness	0.0032	m
Nominal flow rates	5,82-145,50	l/h

The main characteristics of the recirculation pump of the storage bypass loop, which is a Verderflex OEM M3000, is summarized in Table 5.

Table 5. Specifications of the Verderflex OEM M3000 pump.

Specification	Value	M.u.
Power consumption	100	W
Protection rating	IP66	-
Speed control	setted	-
Speed possibilities	55 or 125 or 240	RPM
Standard tube material	verderprene	-
Standard tube inner diameter size	0.0096	m
Standard tube inner diameter thickness	0.0032	m
Nominal flow rates	46,9 or 106,5 or 204,5	l/h

Figure 7 Full scale prototype: peristaltic pump.

4.5 Demand Side Simulator (DSS)

In order to be able to test the prototype under realistic boundary conditions, a suitable DSS was designed. A controlled water flow rate is used to extract, at a controllable rate, the thermal energy stored in the tank. A set of heating demand profiles was defined (over time) by means of

dynamic simulations. Since the size of the prototype was chosen to be scalable, in relation to a typical single family application, a three -zone apartment, served by radiant panels, was adopted for the numerical simulation. The calculations were performed in the same location as the test site and for an entire heating season considering a typical meteorological year. A part of the heating demand profile is reported in Figure 8. The results of the calculations were normalized into a schedule that could be used as input in the prototype control system. In particular:

- the water flow rate is controlled in order to meet the required heating demand;
- the water temperature, at the storage inlet, is adjusted by means of a three-way valve.

This configuration was adopted in order to be able to extract the desired thermal energy from the storage tank with a water flow rate whose temperature is similar to the return temperature of a real radiant panel heating system.

As a result of the numerical modeling of the DSS, a first assessment of the matching between the energy demand for space heating and the energy supply from the solar system was made. As can be seen in Figure 8, where the daily energy production from solar thermal (blue) and the energy demand for space heating (red) values are plotted for all the days of the heating season, the production is much higher than the demand at the beginning and end of the season, while the demand is equal to or higher than the production from December to February.

Figure 8 Example of the plant loop heating demand profile (December and January months).

Figure 9 Profiles of the daily energy demand for space heating and of the daily energy production from solar thermal.

3. Control strategies of the system

The real-scale prototype needs to be controlled using appropriate strategies. Two set of controllers have been identified:

- one regulates the primary loop of the solar collector
- the other manages the discharge of the energy stored in the storage tank.

The latter controller can be operated with two different aims. If the goal of the test is to analyse the performance of the overall solar system during actual operative conditions, the controller reproduces the time profile of the heating DSS described in the previous section (controlling both the water flow rate and the inlet temperature of the water at the storage tank). If the goal of the experiment is only the characterisation of the instantaneous efficiency of the solar collector, the controller acts by instantaneously removing the same heat flux that is "injected" into the puffer by the primary loop from the storage tank.

A more detailed description of the controller logic and of the control strategies is provided in the following sections. The following sections refer to the controlling and monitoring elements of the system that are shown in Figure 9.

5.1 Control strategies for the solar collector loop

Control C1. This is the main controller for the primary loop that includes the solar collector. The fundamental idea of this solar system is to exploit the latent heat as much as possible, in order to maximise the overall energy efficiency of the system [49]. For this reason, the optimal

working condition of the solar collector is the one in which the mPCS concludes its transition phase exactly at the collector outlet. In this way, it is possible to maintain the lowest possible average working temperature of the solar panel (thus minimizing the losses) while still optimizing the thermal energy storage (since the heat for the isothermal phase change is fully exploited). From a practical point of view, this situation occurs when the outlet temperature of the heat carrier fluid is equal to the upper temperature of the melting range, T_{TC7}.

Therefore, the logic that drives this controller is as follows: the temperature of the heat carrier fluid is detected at the outlet of the solar collector and is used as input in a PID system that adjusts the RPM speed of the peristaltic pump (PP1) in order to keep such a temperature as close as possible to the set point fixed at the T_{TC7} value. This temperature was choosen equal to 40 °C (e.g. 3 °C higher than the nominal melting temperature of the mPCM) in the full-scale prototype.

Control C2. This control loop it is used to manage the coupling between the solar collector and the storage tank. Specifically, it avoids the necessity of feeding the puffer with a fluid that is colder than the storage itself. For this reason, the mean temperature (T_{avg}) of seven thermocouples located inside the storage is measured and compared with the temperature at the panel outlet T_{TC7}. If $T_{avg} > T_{TC7}$, the circulation between the collector and the storage (normal mode) is stopped, and valves V1 and V2 are set in by-pass mode. In order to avoid an excessively rapid switching between the by-pass and the normal mode, the circulation between the collector and the storage is only restored when $T_{TC7} \geq (T_{avg} + 5\ °C)$.

Control C3. This pertains to a safety control. In order to avoid problems due to the decay of the material properties, the mPCS must be kept at a temperature that does not exceed 65 - 70 °C. Moreover, some of the components of the storage tank are designed for a maximum temperature of about 65°C. Therefore, if one of the seven thermocouples inside the storage tank reaches a temperature of 65°C, control C3 switches on. When C3 is activated, the curtain of the solar collector comes down and valves V1 and V2 are set in the by-pass mode. In this way, the hot HTF no longer flows in the storage tank and the temperature in the storage tank decreases. The normal working conditions are restored when all the temperatures recorded by the thermocouples inside the storage tank are lower than a safety value of 60 °C.

5.2 Control strategies for the DSS loop. Instantaneous characterisation of the solar panel.

In order to assess the instantaneous efficiency of the solar thermal panel [4], it is necessary to

eliminate the inertial effects due to the storage tank. For this reason, the enthalpy flux related to the HTF that enters the storage tank from the solar collector must be instantaneously removed from the tank. This is achieved by a proper control of the DSS loop.

The heat power generated by the solar collector can be written as:

$$\dot{Q}_u = \dot{m}_{mPCS} \cdot \left(h_{mPCS,out} - h_{mPCS,in} \right) \quad (1)$$

where $\dot{m}_{PCS}$ is the mass flow rate of the mPCS flowing in the collector, while $h_{PCS,in}$ and $h_{PCS,out}$ are the specific enthalpies of the mPCS evaluated at the inlet and the outlet of the panel, respectively. These can be determined by monitoring the temperatures at the inlet T_{TC19} and the outlet T_{TC8} of the collector and then using the curve that relates the temperature and specific enthalpy of the material [15]. As previously mentioned, this curve depends not only on the chosen mPCM, but also on its concentration. An example of this curve is reported in Figure 3a. Fixing on the x-axis the temperature measured by the thermocouples it is possible to establish the value of enthalpy on the y-axis. This was entered as a “true table” in the control system of the real-scale prototype. In order to remove the entire enthalpy flux from the HFT, the water mass flow rate in the DSS loop must satisfy the following equation:

$$\dot{m}_{H_2O} = \frac{\dot{Q}_u}{c_{p\_H_2O}\left(T_{TC16} - T_{TC18}\right)} = \frac{\dot{m}_{mPCS} \cdot \left(h_{mPCS,out} - h_{mPCS,in} \right)}{c_{p\_H_2O} \cdot \left(T_{TC16} - T_{TC18}\right)} \quad (2)$$

The mass flow rate is measured by means of a Coriolis mass flow meter and is controlled by a PID, which modifies the opening of the V3 valve, using the $\dot{m}_{H_2O}$ value, which is assessed by means of equation (2), as the set point.

5.3 Control strategies for the DSS loop. Simulation of the users

Control C4. This loop is used to simulate the behaviour of the prototype under realistic conditions, when the solar system is coupled to a heating system with radiant panels. In this context, control C4 operates so in order to keep the water temperature at the inlet of the heat exchanger in the storage tank (the DSS) at a temperature of about 28 – 30 °C. This value is the typical return temperature of a real radiant panel heating system. In general, the temperature difference between the supply and return HTF used in radiant panel systems is 5 °C. For this reason, the supply temperature at the inlet of the panel is almost 33 – 35 °C, a value that is totally compatible with the solar energy system. Such a control is implemented by means of a three-way valve (V4), which allows a variable recirculation rate of the water at the outlet of the

DSS. The PID regulates the position of valve V4, in order to keep the temperature of the water measured at the inlet of the storage tank (T_{TC18}) at the set point value of 28 - 30 °C.

Control C5. This control allows the time profile of the heating demand to be reproduced and acts on the DSS. The controlled variable is the enthalpy flux that is subtracted from the storage tank, $\dot{Q}_u$, and the control variable is the water mass flow rate, m_{H2O}.

The shape of the time profiles of the heating demand can be chosen freely by the user and are usually the results of the numerical simulations described in section 4.5.

The inlet temperature in the storage tank (T_{TC18}) is kept at a constant nominal value of 28 – 30 °C by means of the C4 control. Instead, control C5 adjusts the water mass flow rate in the following way:

- at each time step, the value of the $\dot{Q}_u$ that has to be removed from the storage tank is taken from a look-up table (that reproduces the user-defined heating demand profiles),
- based on the knowledge of $\dot{Q}_u$, the water mass flow rate that has to flow in the DSS (to remove $\dot{Q}_u$) is cacualted as:

$$\dot{m}_{H_2O} = \frac{\dot{Q}_u}{c_{H_2O}\left(T_{TC16} - T_{TC18}\right)} \qquad (3)$$

  where T_{TC16} is measured at the outlet of the storage tank.
- The water mass flow rate assessed with equation (3) is then compared with the actual value measured by means of the Coriolis meters; if an error is found, the control acts on valve V3 to try to rule out this difference.

Control C6. In order to always ensure a positive energy extraction from the storage tank (and avoid cooling of the hot water of the DSS, instead of heating), it is necessary to be sure that the temperature of the mPCS in the puffer storage tank is always higher than that water in the DSS loop. Control C6 has exactly this task. It monitors the mean temperature in the storage tank (T_{avg}) and compares it with T_{TC18}. If $T_{TC18} \geq T_{avg}$, the DSS loop is stopped. The control completely closes the V3 valve and stops the circulating pump. When a reasonable temperature difference is again reached, C6 restores the normal operation mode.

Post-print of the article:
Design of a low-temperature solar heating system based on a slurry phase change material (PCS)
by Gianluca Serale, Enrico Fabrizio, Marco Perino
Doi: 10.1016/j.enbuild.2015.06.063 published in *Energy & Buildings*, vol 106 (2015), pp- 44-58

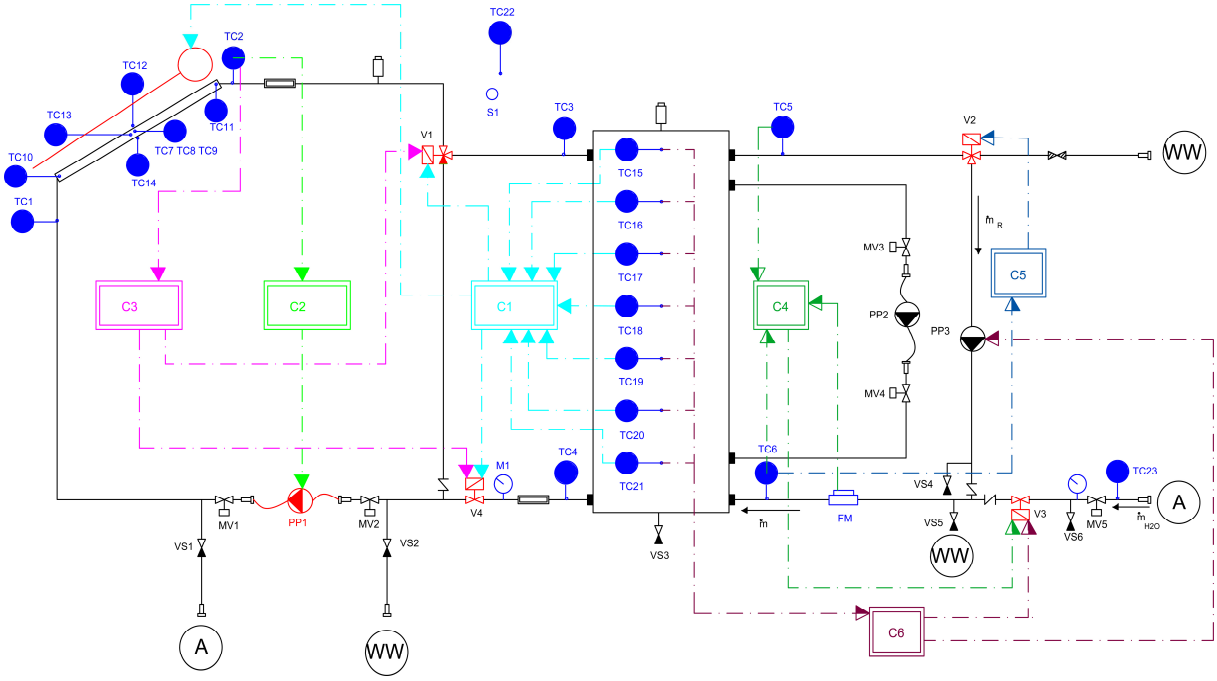

Figure 10 Schematics of the full scale prototype monitoring and control system (A: aqueduct water; C: control; FM: flux meter; M: manometer; MV: manual valve; PP: pump; S: solarimeter; TC: thermocouple; V: electrovalve; WW: waste water).

4. Data acquisition system and design of experiment

The core of the monitoring and control system is a National Instrument Compact RIO with a custom configuration [66]. The acquisition time can be set by the user according to specific requirements (in general for thermodynamic processes the acquisition time is > 1 min). This component allows both the control of the system, following the previously described control logics, and the monitoring of different parameters using specific sensors:

- an IME static wattmeter [67]. This is used to measure the electric power absorbed by the circulation pumps in the PP1 and PP2 primary loops. It has an accuracy of "cl.1", according to the EN/IEC 62053-21 standard, with a resolution of 0.1 kWh. The acquisition frequency is 50 Hz, and it communicates with the rest of the control system using an M-Bus.
- 18 armoured TERSID MTS-15101-T-300 thermocouples [68]. These are T type copper/constantan thermocouples, which are used to monitor and control the temperatures in the different loops of the system.
- a SITRANS FC flow-meter. This is a Coriolis flow meter composed of a flow-rate sensor (MASS 2100) [69] and an electronic transmitter (MASS 6000IP67) [70]. This sensor is used to monitor the water mass flow rate in the DSS. The advantage of using a

Coriolis flow meter is that it directly returns a mass flow rate, and it allows the uncertainty pertaining to the density to be neglected. The nominal declared sensitivity is better than 0.1% of the mass flow rate, and the accuracy on the density is equal to 0.0005 g/cm^3. The MASS 6000IP67 transmitter is combined with the sensor and it delivers exact multiparameter measurements (i.e. mass flow, volume flow, density, temperature and fraction).

- a Campbell Scientific LP02 pyranometer [71]. This was placed next to the panel with the same tilt, in order to monitor the solar incident radiation on the tilted surface. The spectral selectivity is from 305 nm to 2000 nm (+/- 5 %) and the sensitivity is 10-40 μV/Wm^{-2}.

Figure 11 Full scale prototype: thermocouples inserted inside the thermal collector pipes.

The experiments will be carried out for both a traditional heat carrier fluid (that is, a solution of water and glycol) and an mPCS filled system, in order to compare their energy productivity and efficiency.

In particular, the following set of measurements will be conducted:

- assessment of the efficiency of the solar collector (under different working conditions),
- assessment of the overall energy performance of the solar thermal system, taking into consideration both solar energy harvesting and thermal storage,
- analysis of the behavior of the system under various heating energy demand profiles (reproduced by means of the DSS on the basis of the simulated heating profiles).

As far as point a) is concerned, the instantaneous efficiency of the panel will be evaluated on the measured data, using the equation proposed by Duffie et al. [73]:

$$\eta = \frac{\dot{Q}_u}{G_T \cdot A_{collector}} = \frac{\dot{m}_{mPCS} \cdot \left(h_{mPCS,out} - h_{mPCS,in}\right)}{G_T \cdot A_{collector}} \qquad (4)$$

The aim is to gather sufficient data in order to be able to obtain the typical efficiency curve of the solar collector (EU method):

$$\eta_i = \eta_0 - a_1 \cdot \frac{\Delta T_m}{G_T} - a_2 \cdot \frac{\Delta T_m^2}{G_T} \qquad (5)$$

where:

$$\Delta T_m = T_m - T_{outdoor} = \left(\frac{T_{mPCS,out} + T_{mPCS,it}}{2}\right) - T_{outdoor} \qquad (6)$$

The analysis of the efficiency of the whole system (point b), will include the performance assessment of the storage tank and of the energy consumption for the pumps. In fact, thanks to the lower working temperature, the mPCS storage tank is expected to be more efficient than traditional solar thermal systems. On the other hand, the pressure drops caused by the mPCS will be higher than those of the water [74 – 78]. Since an increase in the pressure drops corresponds to an increase in the pump energy consumption, pressure drops need to be limited in order to avoid significantly affecting the benefits derived from the improved thermal efficiency, and the energy demand of the auxiliaries must be investigated in detail.
Finally, in relation to item c), the time mismatch between the energy demand and production will be assessed and the ability of the prototype to reduce such a gap will be verified. In particular, such a study will examine the possibility of "shaving" the heating demand peaks and of optimising the exergy effectiveness. Different demand profiles will be simulated experimentally to stress the storage tank behaviour.

Figure 12 Full scale prototype: general view.

5. Expected results and measurement example

To date, the full scale prototype of the mPCS based solar thermal system has been designed, numerically simulated and built. The debugging activity is underway but some preliminary results, obtained for a water – glycol solution, are available. The monitoring activity is also underway.

As far as the numerical simulations are concerned, a theoretical model that describes the behaviour of the mPCS filled solar collector has been developed by the authors [72], on the basis of the well-known Hotter-Willer (HW) model for traditional flat plate solar collectors [4]. A set of simulations was run to compare the performance of a water-based flat plate solar collector with the performance of an mPCS filled one. From the thermal point of view, the results showed that the mPCS filled solar collector was more efficient than the traditional one [49, 72]. The increase in the mean seasonal efficiency, switching from a water to a mPCS based system, is of about 5 % to 9 %, depending on the boundary conditions. Further benefits that could be obtained from the storage tank have not yet been studied and will be the subject of future numerical and experimental studies.

The aims of the experiments on the full scale prototype are the validation of the numerical models and the assessment of the performance of the overall system, highlighting what the possible benefits of an mPCS based solar thermal system are.

At the moment, the activities are being developed using a 40 % water - glycol solution. This choice is due to two factors. The first, as already mentioned, is that the system can be tested both with a traditional HFT and the innovative mPCS fluid, for comparison purposes.

The second, but not less important reason is that the mPCS tends to present creaming phenomena. Therefore, if the system stops because of some faults, the creaming process could determine clogging problems in the circuit and inside the storage tank. As a consequence, the entire debugging phase has been carried out using a more traditional water glycol solution, which allow the system to be stopped and started at will, without bothering about the sedimentation of the fluid. The mPCS will only be used when the overall hydraulic and control systems have been verified and properly set-up. This will allow the possibilities of a forced stop of the system to be minimized.

It should be recalled that the creaming problem, as previously mentioned, only exists in this development phase, since the phenomenon can be managed properly at a later stage of the research by means of suitable chemical additives.

The first, preliminary, experimental results have been obtained for this winter season. Figure 13 shows, as an example, the time profiles of the inlet and outlet temperatures and the mass flow rate of the HTF in the solar collector. These quantities allow the instantaneous useful energy gain, $\dot{Q}_u$ to be determined (Equation 4).

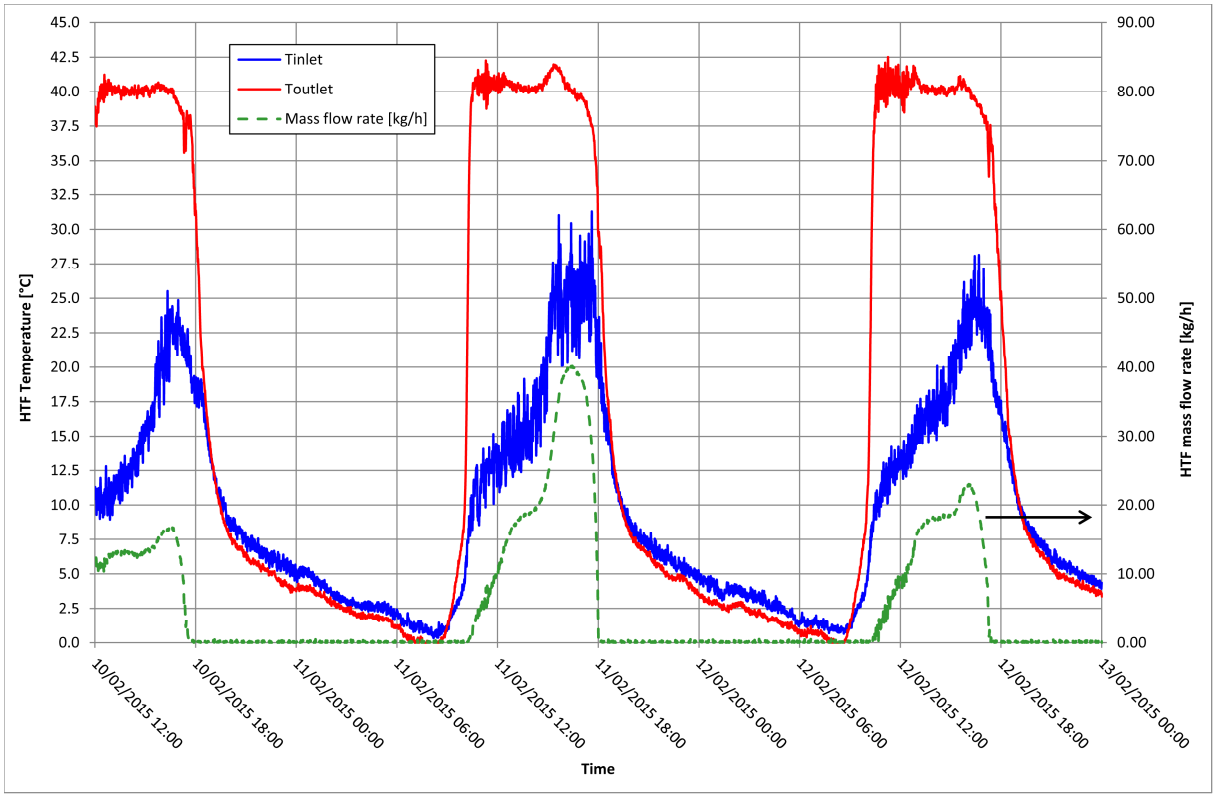

Figure 13 Time profiles of the inlet and outlet temperatures of the HTF and of $\dot{m}_{H_2O}$.

It is worth noting that, for the sake of the commissioning, the system is controlled with the same strategy that will be adopted with the mPCS, that is, the outlet temperature of the HFT is kept constant at set-point value of 40 °C. It is possible to see (Figure 12) the good performance of the control system which, regardless of the boundary conditions, is able to effectively control the outlet temperature of the HFT (that fluctuates between about 40 °C and 42 °C) by properly varying the mass flow rate of the water glycol solution.

The time profiles of the instantaneous useful heat gain, Q_u, are plotted in Figure 14 for three consecutive days, together with the outdoor air temperature and the incident solar radiation. The behaviour of the system confirms the expected trend, with an improvement in the collector efficiency for an increase in the incident solar radiation and in the outdoor air temperature.

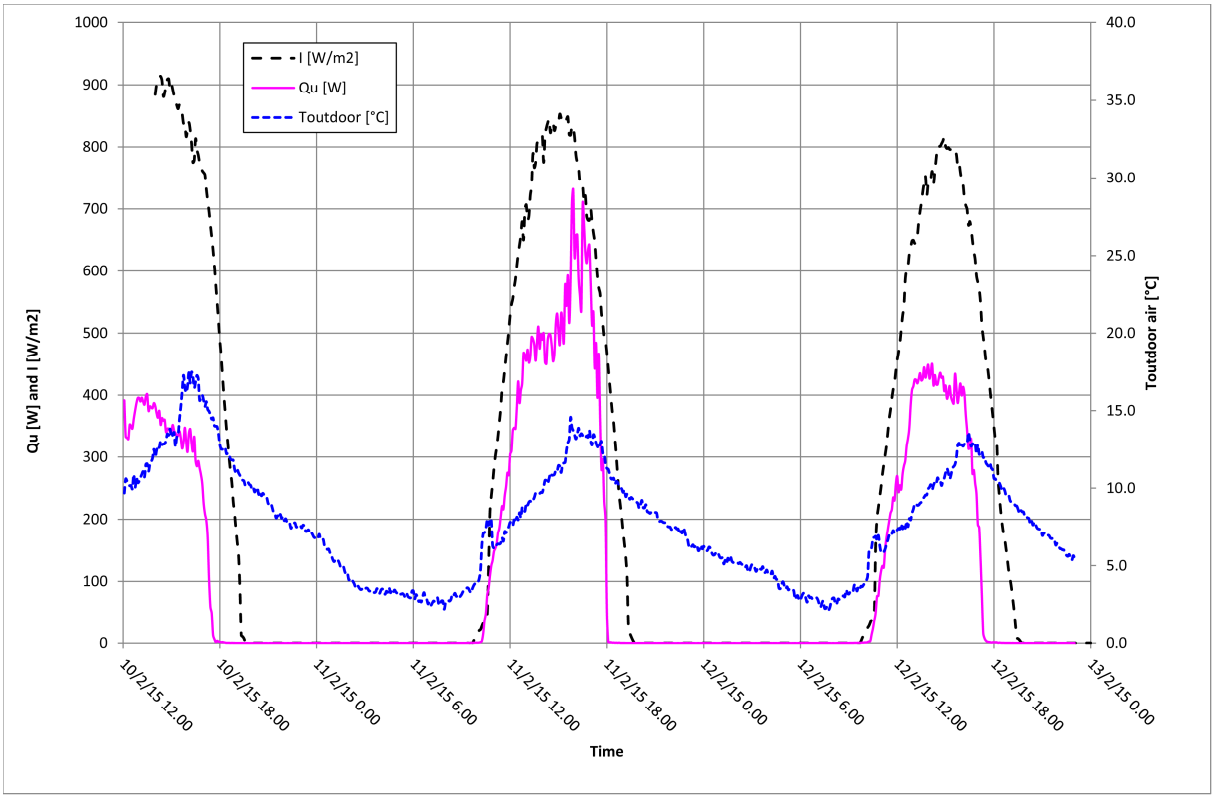

Figure 14 $\dot{Q}_u$ *versus time and boundary conditions (temperature of the outdoor air,* $T_{outdoor}$*, and incident solar radiation,* G_T*)*

The extra-cost of this technology has also been estimated. First, the cost of a standard solar system was estimated equal to 2300 €. This cost takes into account the materials as well as the installation and the manpower costs. The extra costs of the new proposed technical solution were then estimated:

- the cost for the mPCM, which in the present case was equal to 20 €/kg;
- the cost of the peristaltic pump, which can be assumed as 500 €;
- the valves, whose cost can be assumed as 80 € each.

Considering that approximately 90 kg of mPCM was used to fill the primary loop and the 200 l tank with a mixture at 40 wt. %, the cost of the mPCM is 1800 €. Overall, assuming two valves, the extra-cost is 2460 €.However, several considerations should be made at this point. First, the main extra-cost is due to the mPCM, which is currently only produced for special purposes. In the near future, it is likely that with a wider production the cost of an mPCM will be reduced by 50 %; in this case, the extra-cost of the proposed technology would become 1560 €, that is, 68 % of the initial cost. It should also be noted that the extra-costs refers to a system with only one solar collector. Increasing the number of solar collectors, the incidence of the extra-cost on the cost of a standard solar system decreases. Further research should be carried out in order to

increase the performance and reduce these initial extra-costs.

6. Conclusions

An original prototype of a solar thermal system based on mPCS has been conceived, designed and realised. First the system was designed and the pertinent literature was examined. Secondly, a suitable mPCS was chosen and its main thermo-physical properties were examined through different experiments. Each component of the system is described and analysed in this paper, and the particular features of the application and problems emerged during the first stages of the experimental set up are presented. The design of the measurements apparatus and of the control strategies is also introduced and discussed critically. Moreover, the paper illustrates the conception of a DSS that has been tailored to the system from both the numerical modelling and the experimental set-up points of view. Finally, some of the numerical modelling results and of the first experimental results on the performance of the system are shown. Further studies are currently underway concerning an experimental campaign that has been developed in order to study the effect of the thermal storage on the performance of the system under dynamic DSS conditions.

The benefits that can be obtained from the adoption of an mPCS as the HTF are promising. The possibility of operating the collector at lower average temperatures, but still providing a satisfactory enthalpy flux with reasonable mass flow rates, makes it possible to obtain an improvement in the solar panel efficiency and an increase in the exploitation of the solar energy at lower irradiance values.

Moreover, the storage tank can buffer significant thermal energies at a lower temperature, thus reducing the heat losses. Besides, the temperature level of the storage tank (around 40 °C) makes it possible to directly supply the HFT in the terminals of the HVAC system. This further development shows interesting opportunities as far as energy storage is concerned. In fact, the overall extension of the hydraulic network (from the storage tank to the HVAC terminals), filled with the mPCS, may be used as an LHTES device. Such a strategy opens new and interesting scenarios, since it could be possible to exploit a massive, but not cumbersome volume (given the fact that it is already used as a mechanical installation), distributed throughout the entire building. In particular, radiant floor systems offer the best opportunity of taking advantage of such a configuration.

Acknowledgements

This work was carried out within the research project "SolHE-PCM" (2010-2013) funded by the Regione Piemonte (Italy) on ERDF funds in a competitive grant program. Special thanks are due to the industrial partner and co-founder TeknoEnergy for the continuous support in the prototype development.

References

[1] L. Pérez-Lombard, J. Ortiz, C. Pout, A review on buildings energy consumption information, Energy and Buildings 40 (3) (2008) 394–398
[2] T. Kousksou, P. Bruel, G. Cherreau, V. Leoussoff, T. El Rhafiki. PCM storage for solar DHW: From an unfulfilled promise to a real benefit, Solar Energy 85 (2011) 2033–2040.
[3] F. Mauthner, W. Weiss. Solar heat worldwide – market and contributions to the energy supply 2011-2013 edition, SHC programme, international energy agency.
[4] H. Hottel, B. Woertz. Performance of flat-plate solar-heat collectors. Trans. ASME (1942) 64.
[5] V. Verga. Prospettive di sviluppo del solare termico: quali sfide al 2030? 2012, available at www.assolterm.it.
[6] R. Shukla, K. Sumathy, P. Erickson, J. Gong. Recent advances in the solar water heating systems: A review. Renewable and Sustainable Energy Reviews 19 (2013) 173-190.
[7] Y. Raffenel, E. Fabrizio, J. Virgone, E. Blanco, M. Filippi. Integrated solar heating systems: from initial sizing procedure to dynamic simulation. Solar Energy 83 (2009) 657-663.
[8] E. Fabrizio. Energy reduction measures in agricultural greenhouses heating: Envelope, systems and solar energy collection. Energy Build. 53 (2012) 57-63.
[9] P. Pinel, C. Cruickshank, I. Beausoleil-Morrison, A. Wills. A review of available methods for seasonal storage of solar thermal energy in residential applications. Renewable and Sustainable Energy Reviews 15 (2011) 3341–3359.
[10] J. Harrison. The Effects Of Irradiance Level On Thermal Performance Tests Of Solar Collectors Intersol Eighty Five, 1986, pp. 1269-1273.
[11] R.S. Soin, K.S. Rao, D.P. Rao, K.S. Rao. Performance of flat plate solar collector with fluid undergoing phase chance. Solar Energy 23 (1979) 69-73.
[12] A.H. Fanney, C.P. Terlizzi. Testing of refrigerant-charged solar domestic hot water systems. Solar Energy 35 (1985) 353–66.
[13] W.W.S. Charters, V.R. Megler, I. Urma, L. Aye. Propane as working fluid is domestic heat pumps. In: IIR/IIF-Melbourne 1996, Refrigeration, Climate Control and Energy Conversation. 1996 February 11-14. Melbourne, Australia: Melbourne: International Institute of Refrigeration; 1996.
[14] S.D. White, M.G. Yarrall, D.J. Cleland, R.A. Hedley. Modelling the performance of a transcritical CO_2 heat pump for high temperature heating. International Journal of Refrigeration 25 (2002) 479–86.
[15] H. Mehling, L.F. Cabeza, Heat and Cold Storage with PCM: An Up to Date Introduction into Basics and Applications, Springer, 2008.
[16] M. Huang, P. Eames, N. Hewitt. The application of a validated numerical model to predict the energy conservation potential of using phase change materials in the fabric of a building. Solar Energy Materials and Solar Cells 90 (2006) 1951–1960.
[17] F. Goia, M. Perino, V. Serra. Experimental analysis of the energy performance of a full-scale PCM glazing prototype. Solar Energy 100 (2014) 217–233.
[18] M. Pomianowski, P. Heiselberg, Y. Zhang. Review of thermal energy storage technologies based on PCM application in buildings. Energy and Buildings 67 (2013) 56–69.
[19] E. Oró, A. de Gracia, A. Castell, M.M. Farid, L.F. Cabeza. Review on phase change materials (PCMs) for cold thermal energy storage applications. Applied Energy 99 (2012) 513–533.
[20] F. Goia, L. Bianco, Y. Cascone, M. Perino, V. Serra. Experimental Analysis of an Advanced

Dynamic Glazing Prototype Integrating PCM and Thermotropic Layers. Energy Procedia 48 (2014) 1272-1281.
[21] A. Sharma, V.V. Tyagi, C.R. Chen, D. Buddhi. Review on thermal energy storage with phase change materials and applications. Renewable and Sustainable Energy Reviews 13 (2009) 318-345.
[22] Y. Yamagishi, H. Takeuchi, A.T. Pyatenko, N. Kayukawa. Characteristics of microencapsulated PCM slurry as a heat-transfer fluid. AIChE Journal 45 (1999) 696–707.
[23] Y. Rabin, I. Bar-Niv, E. Korin, B. Mikic. Integrated solar collector storage system based on a salt-hydrate phase-change material. Solar Energy 55 (1995) 435-444.
[24] A. Sharma, C.R. Chen. Solar Water Heating System with Phase Change Materials. International Review of Chemical Engineering 1 (2009) 297–307.
[25] J.E. González, N. Dukhan. Initial analysis of PCM integrated solar collectors. Journal of solar energy engineering 128 (2006) 173-177.
[26] E. Mettawee, G. Assassa, Experimental study of a compact PCM solar collector. Energy 31 (2006) 2958–2968.
[27] P.C. Eames, P.W. Griffiths. Thermal behaviour of integrated solar collector/storage unit with 65°C phase change material. Energy Conversion and Management 47 (2006) 3611–3618.
[28] C.S. Malvi, D.W. Dixon-Hardy, R. Crook. Energy balance model of combined photovoltaic solar-thermal system incorporating phase change material. Solar Energy 85 (2011) 1440-1446.
[29] G. Ciulla, V. Lo Brano, M. Cellura, V. Franzitta, D. Milone. A Finite Difference Model of a PV-PCM System. Energy Procedia 30 (2012) 198–206.
[30] D. Haillot, E. Franquet, S. Gibout, J.P. Bédécarrats. Optimization of solar DHW system including PCM media. Applied Energy 109 (2013) 470–475.
[31] D. Haillot, F. Nepveu, V. Goetz, X. Py, M. Benabdelkarim. High performance storage composite for the enhancement of solar domestic hot water systems: Part 2. Numerical system analysis. Solar Energy 86 (2012) 64–77.
[32] S. Canbazoglu, A. Sahinaslan, A. Ekmekyapar, Y.G. Aksoy, F. Akarsu. Enhancement of solar thermal energy storage performance using sodium thiosulfate pentahydrate of a conventional solar water-heating system. Energy and Buildings 37 (2005) 235–242.
[33] L.F. Cabeza, M. Ibanez, C. Sole, J. Roca, M. Nogues. Experimentation with a water tank including a PCM module. Solar Energy Materials & Solar Cells 90 (2006) 1273–1282.
[34] M.J. Huang, P.C. Eames, S. McCormack, P. Griffiths, N.J. Hewitt, N. J. Microencapsulated phase change slurries for thermal energy storage in a residential solar energy system. Renewable Energy 36 (2011) 2932–2939.
[35] K.E. Kasza, M.M. Chen. Improvement of the performance of solar energy or waste heat utilization systems by using phase-change slurry as an enhanced heat-transfer storage fluid. Journal of solar energy engineering 107 (1985) 229-236.
[36] Z. Chen, G. Fang. Preparation and heat transfer characteristics of microencapsulated phase change material slurry: A review. Renewable and Sustainable Energy Reviews 15 (2011) 4624–4632.
[37] M. Delgado, A. Lázaro, J. Mazo, B. Zalba. Review on phase change material emulsions and microencapsulated phase change material slurries: materials, heat transfer studies and applications. Renewable and Sustainable Energy Reviews 16 (2012) 253-273.
[38] Z. Youssef, A. Delahaye, L. Huang, F. Trinquet, L. Fournaison, C. Pollerberg, C. Doetsch. State of the art on phase change material slurries. Energy Conversion and Management 65 (2013) 120-132.
[39] L. Royon, P. Perrot, G. Guiffant, S. Fraoua. Physical properties and thermorheological behaviour of a dispersion having cold latent heat-storage material. Energy conversion and management 39 (1998) 1529-1535.
[40] M. Delgado, A. Lázaro, C. Peñalosa, J. Mazo, B. Zalba. Analysis of the physical stability of PCM slurries. International Journal of Refrigeration 36 (2013) 1648-1656.
[41] H. Inaba. New challenge in advanced thermal energy transportation using functionally thermal fluids. International journal of thermal sciences 39 (2000) 991-1003.
[42] P. Zhang, Z.W. Ma, R.Z. Wang. An overview of phase change material slurries: MPCS and CHS. Renewable and Sustainable Energy Reviews 14 (2010) 598-614.
[43] A. Sciacovelli, F. Gagliardi, V. Verda. Maximization of performance of a PCM latent heat storage

system with innovative fins. Applied Energy 137 (2015) 707-715.
[44] C. Alkan, A. Sarı, A. Karaipekli. Preparation, thermal properties and thermal reliability of microencapsulated n-eicosane as novel phase change material for thermal energy storage. Energy Conversion and Management 52 (2011) 687-692.
[45] Microtek Laboratories, MPCM 37, http://www.microteklabs.com/pdfs/MPCM-37%20Product%20Data%20Sheet.pdf (available at 09/02/2015)
[46] https://www.thermalfluidscentral.org/encyclopedia/index.php/Thermophysical_Properties:_Phase_Change_Materials (available at 09/02/2015)
[47] A. Genovese, G. Amarasinghe, M. Glewis, D. Mainwaring, R.A. Shanks. Crystallisation, melting, recrystallisation and polymorphism of n-eicosane for application as a phase change material. Thermochimica Acta, 443 (2006) 235–244.
[48] B. Chen, X. Wang, Y. Zhang, H. Xu, R. Yang. Experimental research on laminar flow performance of phase change emulsion. Applied thermal engineering 26 (2006) 1238-1245.
[49] G. Serale, S. Baronetto, F. Goia, M. Perino. Characterization and Energy Performance of a Slurry PCM-based Solar Thermal Collector: A Numerical Analysis, in Proceedings of SHC, Freiburg, Germany, 23-25 September 2013.
[50] B. Chen, X. Wang, R. Zeng, Y. Zhang, X. Wang, J. Niu, Y. Li, H. Di. An experimental study of convective heat transfer with microencapsulated phase change material suspension: Laminar flow in a circular tube under constant heat flux. Experimental Thermal and Fluid Science 32 (2008) 1638-1646.
[51] M. Goel, S. Roy e S. Sengupta. Laminar forced convection heat transfer in microcapsulated phase change material suspensions. International Journal of Heat and Mass Transfer 37 (1994) 593-604.
[52] P. Charunyakorn, S. Sengupta e S. Roy. Forced convection heat transfer in microencapsulated phase change material slurries: flow in circular ducts. International Journal of Heat and Mass Transfer 34 (1991) 819-833.
[53] Buttitta, G., Cascone Y., Serale G. (2015). Enthalpy-temperature evaluation of slurry phase change materials with T-history method. Submitted at: International Building Physics Conference 2015 (Turin).
[54] Cabeza, L. F., Barreneche, C., Martorell, I., Miró, L., Sari-Bey, S., Fois, M., ... & Fernández, A. I. (2015). Unconventional experimental technologies available for phase change materials (PCM) characterization. Part 1. Thermophysical properties. Renewable and Sustainable Energy Reviews, 43, 1399-1414.
[55] M.A. Fazilati, A.A. Alemrajabi. Phase change material for enhancing solar water heater, an experimental approach. Energy Conversion and Management 71 (2013) 138-145.
[56] I.M. Bugaje. Enhancing the thermal response of latent heat storage systems. International journal of energy research 21 (1997) 759-766.
[57] A. Trp, K. Lenic, B. Frankovic. Analysis of the influence of operating conditions and geometric parameters on heat transfer in water-paraffin shell-and-tube latent thermal energy storage unit. Applied Thermal Engineering 26 (2006) 1830-1839.
[58] A. Sarı, A. Karaipekli. Thermal conductivity and latent heat thermal energy storage characteristics of paraffin/expanded graphite composite as phase change material. Applied Thermal Engineering 27 (2007) 1271-1277.
[59] G.H. Zhang, C.Y. Zhao. Thermal property investigation of aqueous suspensions of microencapsulated phase change material and carbon nanotubes as a novel heat transfer fluid. Renewable Energy 60 (2013) 433-438.
[60] R. Al-Shannaqa, M. Farida, S. Al-Muhtasebb, J. Kurdic (2015). Emulsion stability and cross-linking of PMMA microcapsules containing phase change materials Solar Energy Materials and Solar Cells, 132, 311-318.
[61] Fernández, A. I., Solé, A., Giró-Paloma, J., Martínez, M., Hadjieva, M., Boudenne, A., ... & Cabeza, L. F. (2015). Unconventional experimental technologies used for phase change materials (PCM) characterization: part 2–morphological and structural characterization, physico-chemical stability and mechanical properties. Renewable and Sustainable Energy Reviews, 43, 1415-1426.
[62] T. Tadros. Application of rheology for assessment and prediction of the long-term physical stability of emulsions. Advances in Colloid and Interface Science 108 (2004) 227-258.
[63] Y. Yamagishi, T. Sugeno, T. Ishige, H. Takeuchi, A.T. Pyatenko, A. T. An evaluation of

microencapsulated PCM for use in cold energy transportation medium. Energy Conversion Engineering Conference, 1996. IECEC 96., Proceedings of the 31st Intersociety, vol. 3, pp. 2077-2083.
[64] J.L. Alvarado, C. Marsh, C. Sohn, G. Phetteplace, T. Newell. Thermal performance of microencapsulated phase change material slurry in turbulent flow under constant heat flux. International Journal of Heat and Mass Transfer 50 (2007) 1938-1952.
[65] S. Gschwander, P. Schossig, H.M. Henning. Micro-encapsulated paraffin in phase-change slurries. Solar Energy Materials and Solar Cells 89 (2005) 307-315
[66] Technical report available at: http://www.ni.com/compactrio (date 30/01/2015);
[67] Technical report available at: http://www.imeitaly.com/docs/02_Static_energy_meters_12.pdf (date 30/01/2015)
[68] Technical report available at: http://www.tersid.it/userfiles/file/TC%20Minia.pdf (date 30/01/2015)
[69] Technical report available at: http://w3.siemens.com/mcms/sensor-systems/en/process-instrumentation/flow-measurement/coriolis-flow-meter/sensors/pages/sitrans-f-c-mass-2100-di-3-40.aspx (date 30/01/2015)
[70] Technical report available at: https://mall.industry.siemens.com/mall/en/WW/Catalog/Products/10020516 (date 30/01/2015)
[71] Technical report available at: http://s.campbellsci.com/documents/cr/manuals/lp02.pdf (date 30/01/2015)
[72] S. Baronetto, G. Serale, F. Goia, M. Perino. Numerical model of a slurry PCM based solar thermal collector. Lecture Notes in Electrical Engineering 263 (2014) 13-20.
[73] J.A. Duffie, W.A. Beckman. Solar engineering of thermal processes. John Wiley & Sons, 2013, pp. 1529-1535.
[74] M. Delgado, A. Lázaro, J. Mazo, J.M. Marín, B. Zalba. Experimental analysis of a microencapsulated PCM slurry as thermal storage system and as heat transfer fluid in laminar flow. Applied Thermal Engineering 36 (2012) 370-377.
[75] A. Heinz, W. Streicher. Application of phase change materials and PCM-slurries for thermal energy storage. In: 10th International Conference on Thermal Energy Storage, 2006.
[76] F. Dammel, P. Stephan. Heat transfer to suspensions of microencapsulated phase change material flowing through minichannels. Journal of Heat Transfer 134 (2012).
[77] Y. Zhang, Z. Rao, S. Wang, Z. Zhang, X. Li, X. Experimental evaluation on natural convection heat transfer of microencapsulated phase change materials slurry in a rectangular heat storage tank. Energy Conversion and Management 59 (2012) 33-39.
[78] G.H. Zhang, C.Y. Zhao. Thermal and rheological properties of microencapsulated phase change materials. Renewable Energy 36 (2011) 2959-2966.